Doctoral Dissertation

Bactericidal effect of cationic hydrogels prepared from hydrophilic polymers

(親水性高分子から調製したカチオン性ハイドロゲルの殺菌効果に関する研究)

By

Yuki Shibata

Supervisor: Takayuki Kurokawa,

HOKKAIDO UNIVERSITY

Laboratory of Soft & Wet Matter,

Graduate School of Life Science, Hokkaido University

Sapporo 001-0021, Japan

September, 2020

CHAPTER 1: General introduction

Hydrogel is a material which forms a three-dimensional network using a highly hydrophilic polymer as a main chain. Hydrogels change their charge depending on the polymer they are composed of, and many studies have been conducted using their properties.[1-5.] In addition, hydrogels are hydrated polymeric materials usually comprising >90% water by weight. Hydrogels are used in products such as contact lenses and form the basis of cellular structure.[6-8] Furthermore, hydrogels have been assessed for their various biomedical applications[9-11] However, hydrogels are susceptible to bacterial contamination owing to their high water content and application in humid environments.

It is very important to prevent bacterial contamination, numerous studies have focused on the antibacterial properties of hydrogels. Numerous recent studies have focused on the incorporation of bactericidal substances including silver nanoparticles [12-15] and chitosan [16-20] into hydrogels. At present, many materials with bactericidal effects have been discovered, and their mechanisms are also diverse. Bactericidal mechanisms can be broadly divided into two. One is the mechanism by which germicides enter bacteria and inhibit their metabolism. An example is penicillin. Penicillin binds to and inhibits the cell wall peptidoglycan forming enzyme (PBP)[21,22]. As a result, the bacterium is

unable to form a cell wall and the cell wall gradually becomes thinner. The difference in osmotic pressure between the inner cytoplasm and the outer fluid causes the bacteria to expand and eventually rupture. The other is a mechanism by which a hole is made in the cell membrane of a bacterium by physical action to kill bacteria. In recent years, it has been clarified that the wing of cicada has such a sterilization mechanism. Microscopic examination of the cicada's wings revealed numerous nano-sized pillars on its surface. When bacteria come into contact with the pillar, the pillar penetrates the bacteria. The cell membrane is pulled by the pillars, which eventually rupture and kill the bacteria. [23-26]

Heavy use of microbicides that block metabolism in bacteria, such as penicillin, risks the bacteria developing resistance to the drug. In fact, penicillin-resistant Streptococcus pneumoniae (PRSP) was known as a bacterium which acquired resistance to penicillin.[27,28]

PRSP has a mutation in the penicillin-binding protein that is the target of penicillin, so penicillin does not work. In this way, drug-resistant bacteria make the drug ineffective by mutating the drug's target protein or by creating a drug efflux pump.[29] Infections with drug-resistant organisms are difficult to treat and increase the risk of serious illness and death. On the other hand, the physical sterilization mechanism such as nano pillar attracts

attention because of the merit that bacteria are difficult to acquire resistance.

Some fungicides do not enter the cell but act directly on the cell membrane. One of these is biguanide fungicides. Biguanide has a cationic functional group and numerous studies have focused on its bactericidal effect. [30-34] These groups bind to the phospholipid head groups of the anion-charged plasma membrane through ionic interactions. Binding of biguanide fungicides to phospholipids on the outer leaflets of the plasma membrane is believed to impair membrane fluidity. The attached region gradually forms a domain and then separates from the plasma membrane. Cytoplasm leaks from this site, eventually killing the bacteria. Substances displaying their activity on the surface of plasma membranes, such as biguanide bactericide, are not affected by drug-resistant bacteria with resistance mechanisms through drug efflux pumps. [35,36]

In this paper, we focused on the bactericidal mechanism of biguanide fungicides and evaluated the bactericidal effect of hydrophilic cationic hydrogels contain numerous cationic groups bound to the polymer. These groups bind with phospholipids in the outer leaflet of the plasma membrane, forming a polyelectrolyte complex. Similar to biguanide bactericide, we expected that the cell membrane is disrupted at its poorly fluid domain formed by cationic hydrogels and the bacteria are killed. Hydrophilic cationic hydrogels are environmentally compatible materials because they do not

contain sustained release bactericides. Furthermore, this substance would not result in bacterial resistance, since mechanisms underlying its bactericidal action involve the destruction of cell membranes externally and do not involve the expression of drug efflux pumps.

In Chapter 2, we described the synthesis methods and compositions of the hydrogels used in this study, the types and culture methods of the bacteria used in the sterilization test.

In Chapter 3, we examined the time required to sterilize cationic hydrogels. The bacteria were seeded on a hydrogel, and the survival of the bacteria was observed by time laps. Before observation, the hydrogel was impregnated with a fluorescent dye (SYTO -9) that could stain live bacteria and a fluorescent dye (Propidium iodide) that could stain dead bacteria.[37] The life and death of the bacterium can be distinguished by the fluorescence microscope observation. One place of the hydrogel surface was time-lapsed observed by fluorescence microscopy. The survival curve was prepared by calculating the survival rate of the bacteria at every elapsed time. Agar was used as a negative control. As the result, it was clarified that the cationic hydrogel showed the sterilization effect by contacting

with the fungus for a long time.

In Chapter 4, three substrates were prepared: cationic hydrogel, neutral hydrogel, and agar, on which bacteria were seeded. After the substrate was placed in an incubator for a certain period of time, the microscopical observation was performed to calculate the survival ratio of the bacteria. The bactericidal effect of cationic hydrogels was evaluated by comparing the survival ratio between substrates. Next, in order to clarify whether the bactericidal effect observed over time was unique to PDMAPAA-Q gel, several cationic hydrogels (Crosslinking agent concentration: 6 mol%) with different monomer species were prepared and the same bactericidal tests were performed on the cationic hydrogels. The results showed that the cationic hydrogels showed high bactericidal activity in spite of their different chemical structures.

In Chapter 5, we examined which factors in cationic hydrogels were associated with bactericidal effects. Copolymer hydrogels were formed from neutral and cationic monomers and their bactericidal effects on *E. coli* were investigated. The hydrogel having different physicochemical properties was prepared by adjusting the ratio of the cationic monomer constituting the hydrogel and the concentration of the crosslinking

agent. In this study, the correlation between the initial elastic modulus, the areal density of cationic monomer unit, and the water content and the mortality ratio of bacteria was investigated. The results showed a strong correlation with the areal density of cationic monomer unit.

In Chapter 6, we investigated whether PDMAPAA-Q has a bactericidal effect even in the uncrosslinked polymer state. The results showed that the death ratio of E. coli in cationic polymer solutions was less than 40%. Furthermore, the death ratio of *E. coli* in cationic polymers was compared with that of E. coli on cationic hydrogels. As the result, it was clarified that the cationic polymer made from the same monomer species showed high bactericidal effect by crosslinking.

In Chapter 7, we calculated the elastic energy of cationic hydrogels and the interfacial energy of bacterial cell membranes and discussed the bactericidal mechanism of cationic hydrogels from these values. The results showed that the elastic energy increased as the area of adhesion between the bacteria and the cationic hydrogel increased, eventually exceeding the interfacial tension of the cell membrane. These results suggest that the cationic hydrogel makes extensive contact with bacteria by ionic interactions, destroys

the cell membrane by the elastic energy generated there.

Finally, in Chapter 8, the conclusion of this research were summarized.

1.1 References

(1) Maria, A. B.; Laura, D.; Agata, G.; Monica, F. V; Anna, C.; Suzuki, S.; Pierfrancesco, C. The effect of the surface charge of hydrogel supports on thermophilic biohydrogen production. Bioresource Technology 2010, 101 (12), 4386–4394.

(2) Yang, J.; Xiao, Y.; Tang, Z.; Luo, Z.; Li, D.; Wang, Q.; Zhang, X. The negatively charged microenvironment of collagen hydrogels regulates the chondrogenic differentiation of bone marrow mesenchymal stem cells in vitro and in vivo. J. Mater Chem B. 2020, doi: 10.1039/d0tb00172d.

(3) Soltys-Robitaille CE,; Ammon, DM, Jr; Valint, PL, Jr,; Grobe, GL, 3rd The relationship between contact lens surface charge and in-vitro protein deposition levels. Biomaterials 2001, 22 (24), 3257–60.

(4) Tao Lin Sun,; Takayuki, K.,; Shinya, K.,; Abu, Bin, Ihsan,; Taigo, A.,; Koshiro, S.,; Md. Anamul, Haque,; Tasuku, N.,; Jian, P. G. Physical hydrogels composed of

polyampholytes demonstrate high toughness and viscoelasticity. Nature Materials 2013 12 (10), 932-937.

(5) Feng, L.; Tao Lin Sun; Tasuku, N.; Takayuki K.; Yu, Z.; Koshiro, S.; Abu Bin Ihsan; Xufeng, L.; Honglei, G; Jian, P. G. Oppositely Charged Polyelectrolytes form Tough, Self-healing and Rebuildable Hydrogels. Advanced Materials 2015 27 (17), 2722-2727.

(6) Chaudhuri, O.; Viscoelastic hydrogels for 3D cell culture. Biomaterials Sci. 2017 5, 1480.

(7) Dosh, R.H.; Jordan-Mahy, N.; Sammon C.; Le, C.L. Use of l-pNIPAM hydrogel as a 3D-scaffold for intestinal crypts and stem cell tissue engineering. *Biomater. Sci.* 2019 7, 4310.

(8) Hyland, L.L.; Twomey, J.D.; Vogel, S.; Hsieh A.H.; Yu, Y.B.; Enhancing biocompatibility of D-oligopeptide hydrogels by negative charges. *Biomacromolecules* 2013 *14*, 406-412.

(9) Naahidi, S.; Jafari, M.; Logan, M.; Wang, Y., Yuan, Y.; Bae, H.; Dixon B.;

Chen, P. Biocompatibility of hydrogel-based scaffolds for tissue engineering applications. *Biotechnol. Adv.* 2017 *35 (5)*, 530-544.

(10) Ye, Y.N.; Frauenlob, M.; Wang, L.; Tsuda, M.; Sun, T.L.; Cui, K.; Takahashi, R.; Zhang, H.J.; Nakajima, T.; Nonoyama, T.; Kurokawa, T.; Tanaka S.; Gong, J.P. Tough and Self‐Recoverable Thin Hydrogel Membranes for Biological Applications. *Adv. Funct. Mater.* 2018 *28 (31)*, 1.

(11) Drury J.L.; Mooney, D.J. Hydrogels for tissue engineering: scaffold design variables and applications. *Biomaterials* 2003, *24*, 4337-4351.

(12) Murali Mohan, Y.; Lee, K.; Premkumar T.; Geckeler, K.E. Hydrogel networks as nanoreactors: A novel approach to silver nanoparticles for antibacterial applications *Polymer* 2007 *48 (1)*, 158-164

(13) Li, M.; Jiang, X.; Wang, D.; Xu Z.; Yang, M. In situ reduction of silver nanoparticles in the lignin based hydrogel for enhanced antibacterial application. *Colloid Surface B*. 2019, *177*, 370-376.

(14) Carmen, C. Pairas; Clare, S. Mahon; David, K. Smith Self-assembled supramolecular hybrid hydrogel beads loaded with silver nanoparticles for antimicrobial application. *Chemistry A European Journal* 2020, doi: 10.1002/chem.202001349.

(15) Fan, L.; Xie, J.; Zheng, Y.; Wei, D.; Yao, D.; Zhang, J.; Zhang, T. Antibacterial, Self-Adhesive, Recyclable, and Tough Conductive Composite Hydrogels for Ultrasensitive Strain Sensing. *ACS Appl. Mater. Interfaces* 2020 12(19), 22225-22236.

(16) Ding, F.; Nie, Z.; Deng, H.; Xiao, L.; Du Y.; Shi, X. Antibacterial hydrogel coating by electrophoretic co-deposition of chitosan/alkynyl chitosan. *Carbohydr. Polym.* 2013, *98*, 1547-1552.

(17) Noppakundilograt, S.; Sonjaipanich, K.; Thongchul N. Syntheses, characterization, and antibacterial activity of chitosan grafted hydrogels and associated mica-containing nanocomposite hydrogels. *J. Appl. Polym. Sci.* **2013** *127*, 4927-4938

(18) Lim, S.-H.; & Hudson, S. M. Review of chitosan and its derivatives as antimi-crobial agents and their uses as textile chemicals. Journal of Macromolecular Science,

Part C: Polymer Reviews, 2003 43(2), 223–269.

(19) Li, P.; Poon, Y. F.; Li, W.; Zhu, H.-Y.; Yeap, S. H.; Cao, Y. A polycationic antimicrobial and biocompatible hydrogel with microbe membrane suctioning ability. Nature Materials 2011 10(2), 149–156.

(20) Rabea, E. I.; Badawy, M. E. T.; Stevens, C. V.; Smagghe, G.; Steurbaut, W. Chitosan as antimicrobial agent: Applications and mode of action. Biomacro- molecules, 2003 4 (6), 1457–1465.

(21) P.M. Blumberg & J. Strominger Interaction of penicillin with the bacterial cell: penicillin-binding proteins and penicillin-sensitive enzymes. Bacteriol. Rev., 1974 38 (3) 291-335.

(22) B.G. Spratt The mechanism of action of penicillin. *Science Progress*, 1978 65 (257) 101-128.

(23) Ting, D.; Nilofar, F.; Terje, S.; Baptiste, L.; Howard F. J. Cicada-inspired cell-instructive

nanopatterned arrays. *Scientific Reports*. 2014 *4*,7122.

(24) Mary, N. D.; Elena, I. L.; Luis, A. R.; Nicolas, V.; Alnert F. Y. Nanopatterned polymer surfaces with bactericidal properties. Biointerphases. **2015** *10 (2)*, 021010.

(25) Sergey, P.; Jafar, H.; Vladimir, A. B.; Hyaden, K. W.; Vi K. T.; The Hong, P. N.; Veselin, B.; Christopher, J. F.; Gregory, S. W.; Jolanta A. W.; Russell, J. C.; Elena, P. I. Biophysical Model of Bacterial Cell Interactions with Nanopatterned Cicada Wing Surfaces. Biophysical journal 2013 *104 (4)*, 835-840.

(26) Jenkins, J.; Mantell, C. N.; Gholinia, A.; Verkade, P.; Nobbs, A. H.; Su, B. Antibacterial effects of nanopillar surfaces are mediated by cell impedance, penetration and induction of oxidative stress. Nature communications **2020** *11*, 1626.

(27) Villanova, Pa. Methods for dilution antimicrobial susceptibility tests for bacteria that grow aerobically. Approved standard M 7-A 3. National Committee for Clinical Laboratory Standerds. 1993.

(28) Klugman, K. P. Pneumococcal resistance to antibiotics. Clin Microbiol Rev 3

1990, 171-196

(29) Hasdemir, U. The role of cell wall organization and active efflux pump systems in multidrug resistance of bacteria. Mikrobiyoloji Bulteni. 2007 *41 (2)*, 309-327.

(30) Chawner, J.A. A comparative study of the bactericidal and growth inhibitory activities of the bisbiguanides alexidine and chlorhexidine *J. Appl. Bacteriol.* 1989, *66*, 243.

(31) Ikeda, T., Tazuke S.; Watanabe, M. Interaction of biologically active molecules with phospholipid membranes. I. Fluorescence depolarization studies on the effect of polymeric biocide bearing biguanide groups in the main chain. Biochim. Biophys. Acta 1983 735 (3), 380

(32) Broxton, P.; Woodcock, P. M.; Gilbert, P. A study of the antibacterial activty of some polyhexamethylene biguanides towards Escherichia coli ATCC 8739. *J. Appl. Bacteriol.* 1983, *54*, 345-353.

(33) Kramer, A.; Eberlein, T. Re-evaluation of polihexanide use in wound

antisepsis in order to clarify ambiguities of two animal studies. *J. Wound Care* 2019 *28(4)*, 246-255.

(34) Hornschuh, M.; Zwicker, P. Schmidt, T. In vitro evaluation of contact-active antibacterial efficacy of Ti-Al-V alloys coated with the antimicrobial agent PHMB. *Acta Biomater.* 2020, doi: 10.1016/j.actbio.2020.02.016.

(35) Gilbert P.; Mcbain, A.J. Potential Impact of Increased Use of Biocides in Consumer Products on Prevalence of Antibiotic Resistance. *Clin. Microbiol. Rev.* 2003, *16*, 189-208.

(36) Gilbert P.; Moore, L.E. Cationic antiseptics: Diversity of action under a common epithet *J. Appl. Microbiol.* 2005 *99 (4)*, 703-715.

CHAPTER 2: Material

2.1 Materials

Three types of cationic hydrogels, a neutral hydrogel, copolymer hydrogels of cationic and neutral monomers, and an agar gel were used herein. The three types of cationic hydrogels were polymerized from (3-acrylamidopropyl) trimethylammonium chloride (DMAPAA-Q) (Tokyo Chemical Industry Co., Ltd.), acryloyloxyethyltrimethylammonium chloride (DMAEA-Q) (Toagosei Co., Ltd.), and 3- (methacryloylamino) propyltrimethylammonium chloride (MPTC) (FUJIFILM Wako Pure Chemical Corporation). The neutral hydrogel was polymerized from N, N-dimethylacrylamide (DMAAm) (FUJIFILM Wako Pure Chemical Corporation). The copolymer hydrogels were polymerized from DMAPAA-Q and DMAAm. N, N '-methylenbis (acrylamide) (MBAA) (FUJIFILM Wako Pure Chemical Corporation) and used as a cross-linker. α-Ketoglutaric acid (α-keto) (FUJIFILM Wako Pure Chemical Co., Ltd.) was used as an initiator. The chemical structures of the three cationic polymers and the neutral polymer PDMAAm are shown in Figure 1. The agar gel was prepared using agar powder. (FUJIFILM Wako Pure Chemical Corporation).

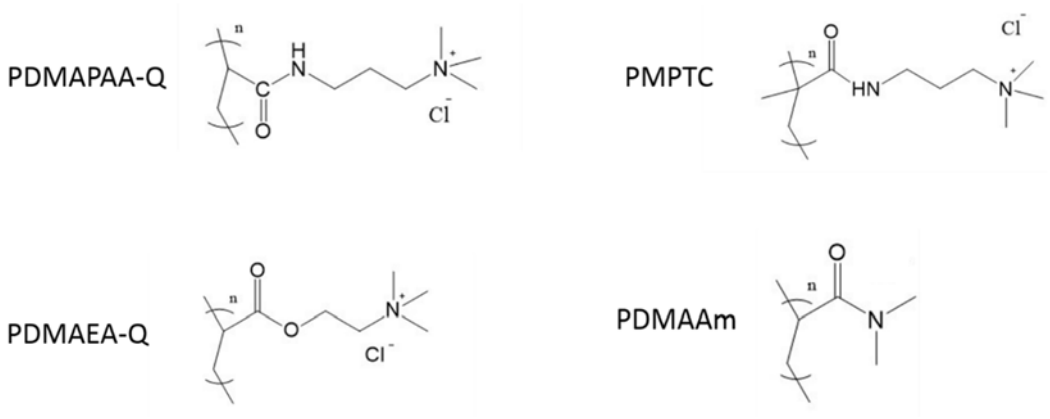

(Figure. 1) Chemical structures of the polymers of the hydrogel used in this study.

2.2 Live/dead® baclight™ bacterial viability kit

Bacteria were stained using a live/dead baclight™ bacterial viability kit(Molecular probes, City of Eugene, USA.) [1-4] in accordance with the manufacturer's instructions, and their viability on the gel was assessed. The kit comprised two fluorochromes: SYTO -9 and propidium iodide (PI). SYTO -9 penetrates the bacterial cell membrane and fluorescently stains live bacteria green (em: 480 nm/ex: 500 nm). PI, which does not permeate the cell membrane, does not fluorescently stain live bacteria. Thus, PI only fluorescently stains dead bacteria with defects in the plasma membrane (em: 490 nm/ex: 635 nm). [5] These fluorochromes were added in physiological saline. Hydrogels were immersed in physiological saline containing fluorescent dyes overnight before seeding.

2.3 Preparation of hydrogels

Hydrogels were prepared through radical polymerization of each monomer and crosslinking agent. When the hydrogel was polymerized, the total monomer concentration was set at 2 M. The concentration of crosslinking agent MBAA and initiator α-keto, monomer, were 2-12 mol% and 0.1 mol% relative to that of the monomer, respectively. To synthesize the hydrogel, a reaction cell was fabricated by sandwiching a silicone spacer along the edge between two parallel glass plates. Silicone

spacers of 2–5-mm thickness were used herein. Hydrogels for antimicrobial testing were prepared using 2-mm-thick silicone spacers. Hydrogels for the analysis of the elastic modulus were prepared using 5-mm-thick silicone spacers. The monomer solution prepared herein was poured into the cell and the cell was placed in a glove box filled with argon. The cells were irradiated using a UV lamp (Wavelength, 365 nm; Intensity, 4mW/cm^2) for approximately 8 h. After polymerization, the hydrogel was eliminated from the glass plate and immersed in pure water for 1 week to remove residual substances in the hydrogel. After 1 week, the hydrogels were transferred to physiological saline (0.9 wt%) and immersed for 3 d. The hydrogel was then autoclaved in physiological saline (120 °C, 20 min). After sterilization in an autoclave, the hydrogels for antimicrobial tests were cut into disks (Φ = 25 mm) and immersed in physiological saline supplemented with SYTO9 and PI for 1 d. Hydrogels for the assessment of the elastic modulus were immersed in physiological saline and sterilized in an autoclave.

2.3.1 Contact angle of the water drop on hydrogel

The contact angle was measured for the PDMAPAA-Q hydrogel, PDMAAm hydrogel, and composite hydrogel. The monomer concentration was 2 M, while that of the cross-linking agent MBAA was 10 mol%. Of the polymers constituting composite hydrogel, 60% was a PDMAPAA-Q and 40% was a PDMAAm. Water droplets were dropped onto these hydrogels on measuring the contact angle. Since the contact angles of all hydrogels were within 20°~40°, these hydrogels were confirmed to be hydrophilic (Figure.2).

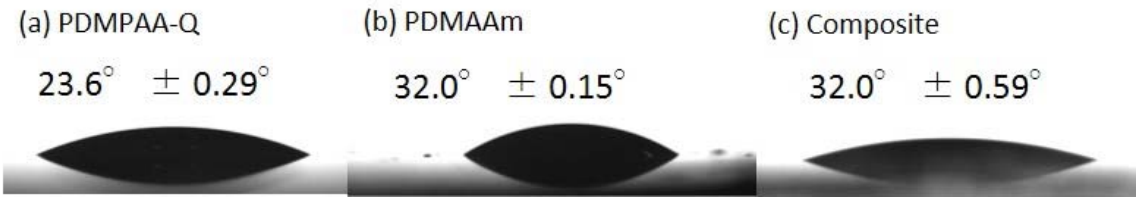

(Figure. 2) Image and contact angle of the water drop on poly (3-acrylamidopropyl) trimethylammonium chloride (PDMAPAA-Q) hydrogel (a), poly N, N-dimethylacrylamide (PDMAAm) hydrogel (b), and Composite hydrogel (c).

2.3.2 Attenuated total reflection (ATR) spectroscopy

Furthermore, ATR measurements were carried out to confirm the presence of cationic functional groups in hydrogels containing cationic polymers (Figure.3)[6,7]. The samples used for this measurement was the same as that used in 5.2. The monomer concentration of the hydrogel was adjusted to 2 M and the crosslinker concentration to 6 mol%. The fraction of cationic monomers in copolymer hydrogel is 0.6.

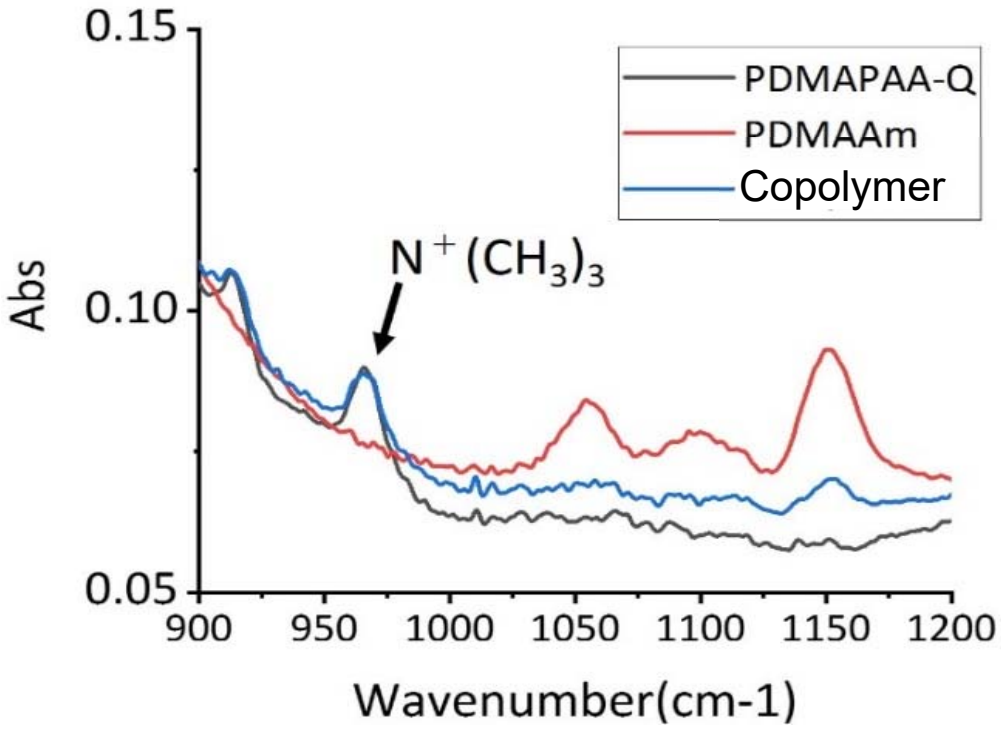

(Figure. 3) Measurement of poly (3-acrylamidopropyl) trimethylammonium chloride (PDMAPAA-Q) hydrogel, poly N, N-dimethylacrylamide (PDMAAm) hydrogel and copolymer hydrogel through attenuated total reflection (ATR) spectroscopy.

2.4 Preparation of bacterial strain

Micrococcus luteus (*M. luteus* NBRC 3333) and *Escherichia coli* (*E. coli* K -12) are used as Gram-positive and Gram-negative strains herein, respectively. Single colonies of *E. coli* were inoculated in liquid Luria-Bertani (LB) medium (Nippon Pharmaceutical Co., Ltd.) and incubated (37 °C) for 1 d. Furthermore, a single colony of *M. luteus* was inoculated on LB medium for 1 d in a shaker incubator (30 °C, 190 rpm). On incubation, the bacterial density (*M. luteus* and *E. coli*) of each bacterium was adjusted to 10^7–10^8 CFU/ml by measuring the turbidity of the bacterial solution, using a spectrophotometer. To eliminate the LB medium from each bacterial suspension, the bacteria were precipitated in a centrifuge (4500 rpm, 10 min, KUBOTA Co., Ltd, Model 4000-), and the supernatant was eliminated. The bacterial pellet was washed with physiological saline and reprecipitated in a centrifuge (4500 rpm, 10 min) to eliminate the supernatant. Washing was repeated thrice to completely eliminate the LB medium. After washing, the bacterial suspension was concentrated 10-fold with physiological saline to increase the bacterial density in the suspension.

2.5 References

(1) Boulos, L.; M. Prevost; B. Barbeau; J. Coallier; and R. Desjardins. LIVE/DEAD BacLight: application of a new rapid staining method for direct enumeration of viable and total bacteria in drinking water. J. Micro- biol. Methods 1999 37, 77–86.

(2) Stocks, S. M. Mechanism and use of the commercially available via- bility stain, BacLight. Cytom. A 2004 61,189–195.

(3) Gasol, J. M.; U. L. Zweifel; F. Peters; J. A. Fuhrman; and A. Hagstrom. Significance of size and nucleic acid content heterogeneity as measured by flow cytometry in natural planktonic bacteria. Appl. Environ. Microbiol. 1999 65, 4475–4483.

(4) Sachidanandham, R.; K. Y. Gin; and C. L. Poh. Monitoring of active but non-culturable bacterial cells by flow cytometry. Biotechnol. Bioeng. 2005 89, 24–31.

(5) Berney, M.; Hammes, F.; Bosshard, F.; Weilenmann H.U.; Egli, T. Assessment and interpretation of bacterial viability by using the LIVE/DEAD BacLight kit in combination with flow cytometry. *Appl. Environ. Microbiol.* **2007** *73 (10)*, 3283-3290.

(6) Bhuyan, M. M.; Okabe, H.; Hidaka, Y.; Hara, K. Pectin-[(3-acrylamidopropyl) trimethylammonium chloride-co-acrylic acid) hydrogel prepared by gamma radiation and selectivelysilver (Ag) metal adsorption. *J. Appl. Polym. Sci.* **2017**, *135*, 45906.

(7) Zheng, H.; Feng, L. Effect of the Cationic Block Structure on the Characteristics of Sludge Flocs Formed by Charge Neutralization and Patching. *Materials* **2017**, *10*, 487.

CHAPTER 3: Time-lapse microscopic observation

3.1 Introduction

As shown in General Introduction, biguanide fungicides with cationic charges show bactericidal activity by contacting the bacterial cell membrane through ionic interactions. First, in this study, in order to investigate whether hydrogels with cationic charge in the main chain have bactericidal effect, bacteria were seeded on cationic hydrogels and their survival was time-lapse microscopic observation. The sterilization time of the cationic hydrogels was determined by calculating the bacterial mortality rate at each elapsed time and creating survival curves.

3.2 Experiments

3.2.1 Materials

Poly (3-acrylamidopropyl) trimethylammonium chloride (PDMAPAA-Q) hydrogel was used as a cationic hydrogel for time-lapse microscopic observation. The concentration of crosslinking agent MBAA and initiator α-keto, monomer, were 6 mol% and 0.1 mol% relative to that of the monomer (2M), respectively. We used agar as a negative control. Agar was shaped to the same shape as the hydrogel and then immersed in saline containing a fluorescent dye for one day before being used for experiments.

3.2.2 Method

The gel was warmed in water at 45℃ before the experiment so that the solution on the gel surface rapidly evaporates. One microliter of each bacterial suspension was seeded on the surface of the warmed gel. The gel seeded with bacteria was placed on a glass dish and observed using a fluorescence microscope equipped with an incubator and a portion of the gel surface was observed with time. Gels seeded with *E.coli* were incubated at 37℃ and those seeded with *M. luteus* were incubated at 30℃. Photographs were obtained every 15 min. Live and dead bacteria were manually enumerated in each image. The survival ratio of bacteria in the images was determined from the number of live bacteria divided by the total number (live and dead) of bacteria and then multiplied by 100. The Bacterial survival ratio at each timepoint was determined and the survival curves of each bacteria were plotted using Origin Pro software. Herein, bacteria were seeded on a nutrient-free substrate. Therefore, the bactericidal properties of the base were evaluated under the condition that the bacteria did not proliferate during the experiment. To eliminate the increased death ratio of *E. coli* on cationic hydrogels owing to natural bacterial death, the death ratio of *E. coli* on hydrogels was corrected using the death ratio of *E. coli* in the negative control.

3.3 Results and Discussion

Time-lapse imaging revealed that almost all *E. coli* cells on agar and cationic hydrogels did not die in a short period (Figure 4). Although only a few *E. coli* cells on agar displayed red fluorescence after 12h, *E. coli* cells on the cationic hydrogel displayed increased red fluorescence with time, and numerous bacterial cells dies after 12 h. The survival ratio of *E. coli* on the PDMAPAA-Q hydrogel was determined from the ratio of the number of green and red fluorescent bacteria in each image (Figure.5). The survival ratio of *E.coli* on after correcting for natural death exponentially decreased with time, following a regression pattern explained using equation (4).

$$y = A\exp(-t/\tau)+y_0 \quad .....(4)$$

where y is the survival ratio, A is the proportional constant, t is the elapsed time (h), τ is the characteristic sterilization time (h), and y_0 is offset. This survival curve reveals that the characteristic sterilization time (τ) of the cationic hydrogel against *E. coli* is approximately 6 h. Furthermore, the survival ratio of *M. luteus* on the gels was determined on the basis of the ratio of the number of green and red fluorescent bacteria in each image (Figure.6). The survival ratio of *M. luteus* on the PDMAPAA-Q hydrogel corrected with the negative control began to rapidly decrease 4 h after seeding. When the fitting curve was plotted after 4 h using equation (4), the value of τ was

approximately 3 h (Figure. 7). Commonly used bactericides exert a bactericidal effect over a short period by degenerating cell membranes or inhibiting bacterial metabolism. Simultaneously, during time-lapse microscopic observation, the cationic hydrogel displayed sterilizing effects by interacting with the bacteria for a long period. Since the present cationic hydrogel does not contain the releasing component, the polymer of the cationic hydrogel interacts with the outer leaflet of the bacterial plasma membrane through long-term interactions, displaying a sterilization effect. The difference in the survival ratio between *E. coli* and *M. luteus* may have resulted from differences in the thickness of the cell wall between gram-negative bacteria (*E. coli*) and gram-positive (*M. luteus*) bacteria. Gram-positive bacteria have a thick cell wall surrounding the plasma membrane, which may have led to the 4-h delay in the interaction between the cationic hydrogel and the bacterial plasma membrane.

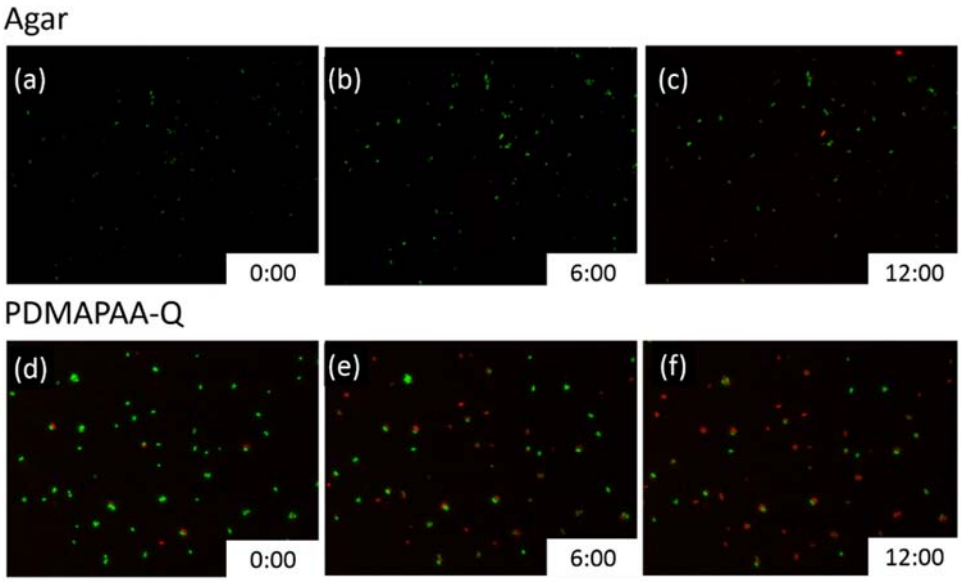

(Figure. 4) Images of live/dead cells on time-lapse fluorescence microscopic observation. Images (a)~(c) show *Escherichia coli* (*E. coli)* on agar and (d)~(f) show *E. coli* on the poly (3-acrylamidopropyl) trimethylammonium chloride (PDMAPAA-Q) hydrogel. (a) and (d) indicate 0 min, (b) and (e) indicate 6 h, and (c) and (f) indicate 12 h after seeding.

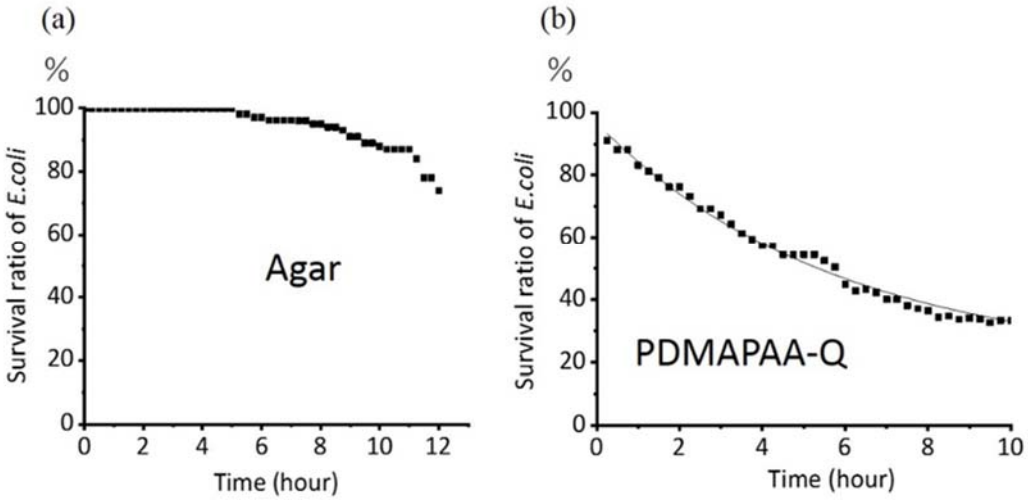

(Figure. 5) Survival ratio of *Escherichia coli* (*E. coli)* on agar gel (a) and the poly (3-acrylamidopropyl) trimethylammonium chloride (PDMAPAA-Q) hydrogel (b). Survival ratio of *E. coli* on PDMAPAA-Q is normalized in graph (a). The characteristic sterilization time (τ) of the PDMAPAA-Q gel to *E. coli was estimated as 6 h.*

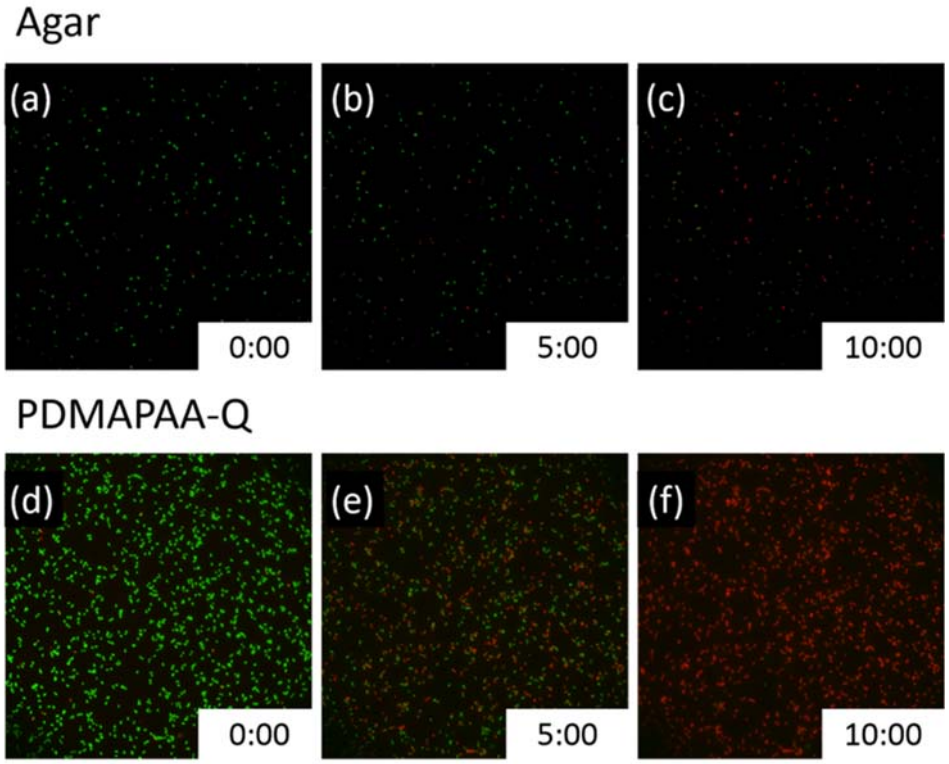

(Figure. 6) Images of live/dead bacteria on time-lapse fluorescence microscopic observation. Images (a)~(c) show *Micrococcus luteus (M. luteus)* on agar. Images (d)~(f) show *M. luteus* on the poly (3-acrylamidopropyl) trimethylammonium chloride (PDMAPAA-Q) hydrogel. Images (a) and (d) indicate 0 min. Images (b) and (e) indicate >5 h. Images (c) and (f) indicate >10 h.

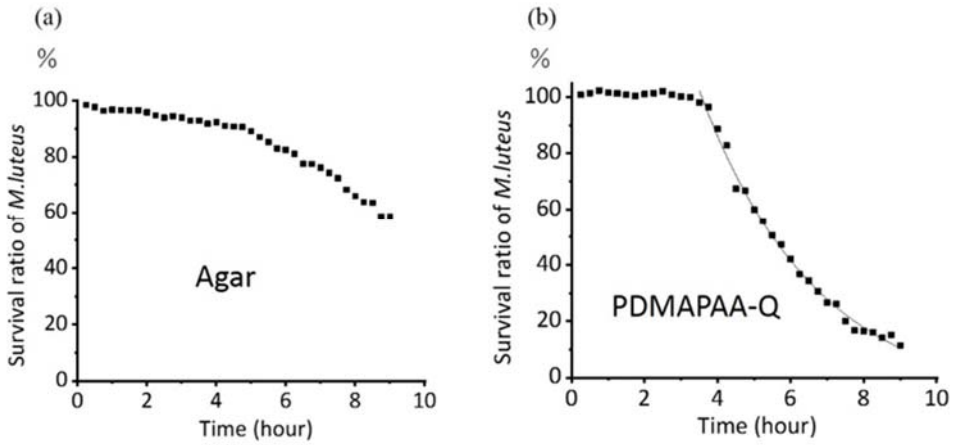

(Figure. 7) Time-lapse observation of *Micrococcus luteus (M. luteus)* on agar (a) and the poly (3-acrylamidopropyl) trimethylammonium chloride (PDMAPAA-Q) hydrogel (b). Survival ratio of *M. luteus* on the PDMAPAA-Q hydrogel was normalized in graph (a). Sterilization of the PDMAPAA-Q hydrogel to *M. luteus was* delayed for 4 h and the characteristic sterilization time [τ] was 3 h. Consequently, the sterilization time was 7 h.

CHAPTER 4: Assessment of the antibacterial effect of the hydrogel

4.1 Introduction

Time-lapse fluorescence microscopic observation revealed that the cationic hydrogel PDMAPAA-Q displayed a sterilization effect upon long-term interaction with the bacteria. Furthermore, we evaluated the effect of charge on the bactericidal properties of the hydrogels.

In Chapter 4, a cationic hydrogel, a neutral hydrogel, and agar were prepared, on which bacteria were seeded. The gels were allowed to stand in an incubator for a period of time, after which the viability of the bacteria on the gel surface was counted by fluorescence microscopy. The bactericidal effect of cationic hydrogels was evaluated by comparing the mortality of bacteria on each gel. Furthermore, several cationic hydrogels with different monomer species (crosslinker density: 6 mol%) were prepared and we examined whether the bactericidal effects observed on time-lapse fluorescence microscopy on *E.coli* are unique to the PDMAPAA-Q hydrogel.

4.2 Experiments

4.2.1 Materials

In this experiment, cationic and neutral hydrogels and agar were used in this experiment. The cationic hydrogels prepared three kinds of cationic hydrogels with different monomer species, respectively. Three kinds cationic monomers, DMAPAA-Q, DMAEA-Q and MPTC, were used to prepare cationic hydrogels herein. Neutral hydrogel was prepared from DMAAm monomer. The crosslinker densities of these hydrogels were prepared at 6 mol%. Two species, *E. coli* and *M. luteus*, were used in the sterilization test.

4.2.2 Method

During time-lapse microscopy, fluorescent dye-containing gels were warmed in warm water at 45 ℃. To prevent the gel from drying out, a wet gauze was placed on a plastic Petri dish and a cover glass was placed over it. The gel was placed on a cover glass and 1μl of a suspension of each bacterium was seeded on the gel surface. In this experiment, two samples were prepared for each hydrogel: one was observed immediately after bacterial inoculation and the other sample was observed after allowing it to stand in an incubator for a certain period. Gels seeded with *E.coli* were placed in an incubator

(37 ℃) for 12 h. Gels seeded with *M. luteus* were placed in an incubator (30 ℃) for 7 h. Bacteria on the gel surface were observed through fluorescence microscopy at Hokkaido University Nikon Imaging Center. Photographs were randomly obtained for 20 fields per gel. Live and dead bacteria were manually enumerated in each image. The death ratio of the bacteria in the photographs was determined using formula (2), where D is the number of dead bacteria and L is the number of live bacteria. To eliminate outliers, the Smirnoff-Grubbs rejection test was performed for the bacterial death ratio. The Bonferroni test was performed to assess significant differences in the bacterial death ratio between the two groups. The bacterial death ratio in the images was determined on the basis of the number of dead bacteria divided by the total number (dead and live) of bacteria and multiplied by 100. As previously reported, bacteria were seeded on a nutrient-free substrate. Therefore, the bactericidal properties of the base were evaluated under the condition that the bacteria did not proliferate during the experiment.

4.3 Results and Discussion

We evaluated the effect of charge on the bactericidal properties of the hydrogels. Cationic hydrogel (crosslinker density: 6 mol%), agar, and a neutral hydrogel (PDMAAm) (crosslinker density: 6 mol%) were prepared, and the antibacterial test was performed. *E. coli* and *M. luteus* were seeded on the gel surfaces, and 20 spots on each gel surface were immediately imaged through fluorescence microscopy after seeding and after a certain period. The bacterial death ratio was determined on the basis of these images. The contact duration between the bacteria and the gel was set to12 h for *E. coli* and 7 h for *M. luteus*, based on the time-lapse observations. The Bonferroni test was performed to determine significant differences between the two groups after a certain period after seeding. The death ratio of *E. coli* was 33.6% for neutral hydrogels, 27.3% for agar, and 86.3% for cationic hydrogels at 12 h after seeding each sample (Figure.8(a)). The death ratio of *E. coli* on the neutral gel was slightly higher than that upon natural death. However, on comparing the cationic hydrogel with the neutral hydrogel, the cationic properties imparted a more prominent bactericidal effect in the cationic hydrogel. In the case of *M. luteus*, the bacterial death ratio on cationic hydrogels was significantly higher than that on agar gel (Figure.8(b)). ($p<0.01$) Furthermore, several cationic hydrogels with different monomer species (crosslinker

density: 6 mol%) were prepared and we examined whether the bactericidal effects observed on time-lapse fluorescence microscopy on *E.coli* are unique to the PDMAPAA-Q hydrogel. In this study, the Dannett's test was performed to assess significant differences in the death ratio of *E. coli* on hydrogels against agar gel. Consequently, the death ratio of *E. coli* on PDMAEA-Q and PMPTC hydrogels 15 min after seeding significantly differed from that of agar (Figure.9). Moreover, after 12 h, the death ratio of *E. coli* on all cationic hydrogels was significantly higher than that in the negative control. These results indicate that cationic hydrogels exhibit high bactericidal activity even though their chemical structures are different.

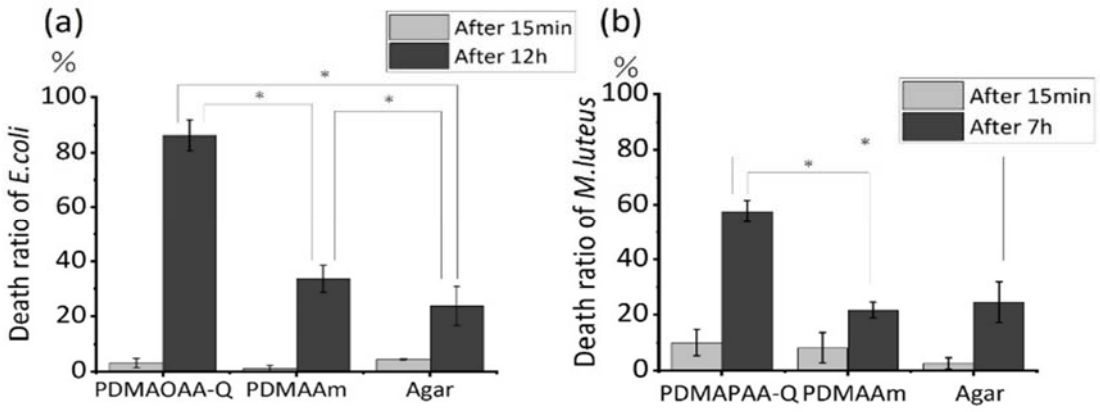

(Figure. 8) The death ratio of (a) *Escherichia coli* (*E. coli)* and (b) *Micrococcus luteus (M. luteus)* on hydrogels and agar after a certain period. Error bars indicate the standard deviation. Significant differences between each sample at 12 h (a) or 7 h (b) after seeding were determined using the Bonferroni test ($p<0.01$).

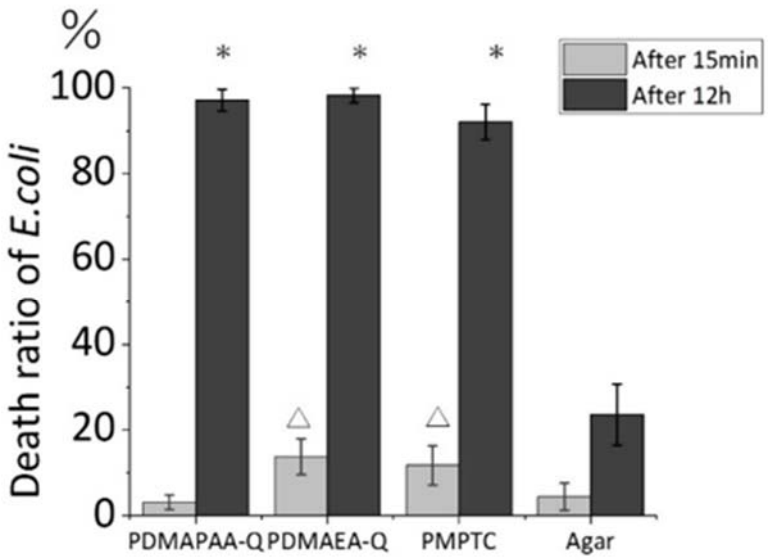

(Figure. 9) Death ratio of *Escherichia coli* (*E. coli)* on cationic hydrogels and agar after a certain period. Error bars indicate the standard deviation. Cationic hydrogel samples after each time point were compared with agar after the same period. Significant differences were observed between the result of agar and other samples, as confirmed via Dunnett's test. ($p<0.01$)

CHAPTER 5: Factors contributing to the antibacterial property of cationic hydrogels

5.1 Introduction

It was revealed that the bactericidal effect was shown by bringing the cationic hydrogel into contact with the fungus in chapter 3 and chapter 4. In chapter 5, to determine which parameter of cationic hydrogels contributes to its bactericidal effects, copolymer hydrogels of cationic and neutral monomers were formed from DMAPAA-Q and DMAAm, and their bactericidal effects on *E. coli* were investigated. Herein, we focused on the effect of the initial elastic modulus, the areal density of the cationic monomer unit, and the water content of these hydrogels on its bactericidal effects. On adjusting the fraction of the cationic monomer constituting the hydrogels and the concentration of the crosslinking agent, hydrogels with different physicochemical properties were prepared. (Figure 10)

5.2 Experiments

5.2.1 Materials

The copolymer hydrogel used in this experiment was prepared from the cationic monomer DMAPAA-Q and the neutral monomer DMAAm. The total monomer

concentration was set at 2 M. The concentration of crosslinking agent MBAA and initiator α-keto, monomer, were 2-12 mol% and 0.1 mol% relative to that of the monomer, respectively. E. coli was used for this antimicrobial test.

5.2.2 Method of antibacterial test

Antimicrobial testing was performed in the same manner as in 4.2. 2.

5.2.3 Measurement of the initial elastic modulus of the hydrogel

The initial elastic moduli of these hydrogels were determined through indentation tests. The force -displacement relationship for each hydrogel was determined using a universal mechanical test apparatus (Tensilon RTC -1310 A: Orientech.) equipped with a hemispherical steel indenter with a 2-mm radius.

The initial elastic modulus (E) of the hydrogel was determined using Equation (1) derived from Hertz's equation. [1-4]

$$f = E\frac{4R^{\frac{1}{2}}}{3(1-{v_P}^2)}l^{\frac{3}{2}} \quad \cdot \quad \cdot \quad \cdot (1)$$

Where, f, l, R, and v_P are the measured force, indenter displacement, indenter radius, and the Poisson's ratio of the hydrogel, respectively. The v_P was 0.5 assuming that the hydrogel volume remains unchanged during the indentation test. The value of E was an

average of 5 measurements. (Figure. 11 (a))

5.2.4 Area density of the hydrogel monomers

The area densities of the hydrogel monomers were determined using the following method. Upon radical polymerization of the hydrogel, the hydrogel thickness t_0 was measured thrice and the average value was determined. The hydrogel was then swollen with physiological saline. Thereafter, the hydrogel was immersed in physiological saline and sterilized in an autoclave (120℃, 20 min). Thereafter, the hydrogel thickness t was determined thrice and the average value was determined. The volume swelling ratio $q=(t/t_0)^3$ was determined on the basis of the changes in thickness, and the "Area density of the monomer" and "Areal density of cationic monomers" s of the hydrogels were determined on the basis of the swelling ratio q and initial monomer concentration C_0 in feed, (Figure. 11 (b))

$s=(C_0/q)^{2/3}$ ...(2)

5.2.5 Determination of the water weight

The water weight of the hydrogels after swelling in saline and sterilization in an autoclave was determined as follows

$$Water\ content\ (\%) = \left(1 - \frac{c_p}{(q-1)d_s + d_g}\right) * 100 \quad ...(3)$$

where q is the volume swelling ratio of the hydrogels swollen in saline, d_s is saline density (1.007 g/ml), d_g is density of the as-prepared gel, and c_p is the polymer concentration (g/ml) in the hydrogel prepared herein. For d_g and c_p, we assume that d_g and c_p were approximately equal to the monomer density and concentration (g/ml) of the precursor solutions of the hydrogels, respectively. (Figure. 11 (c))

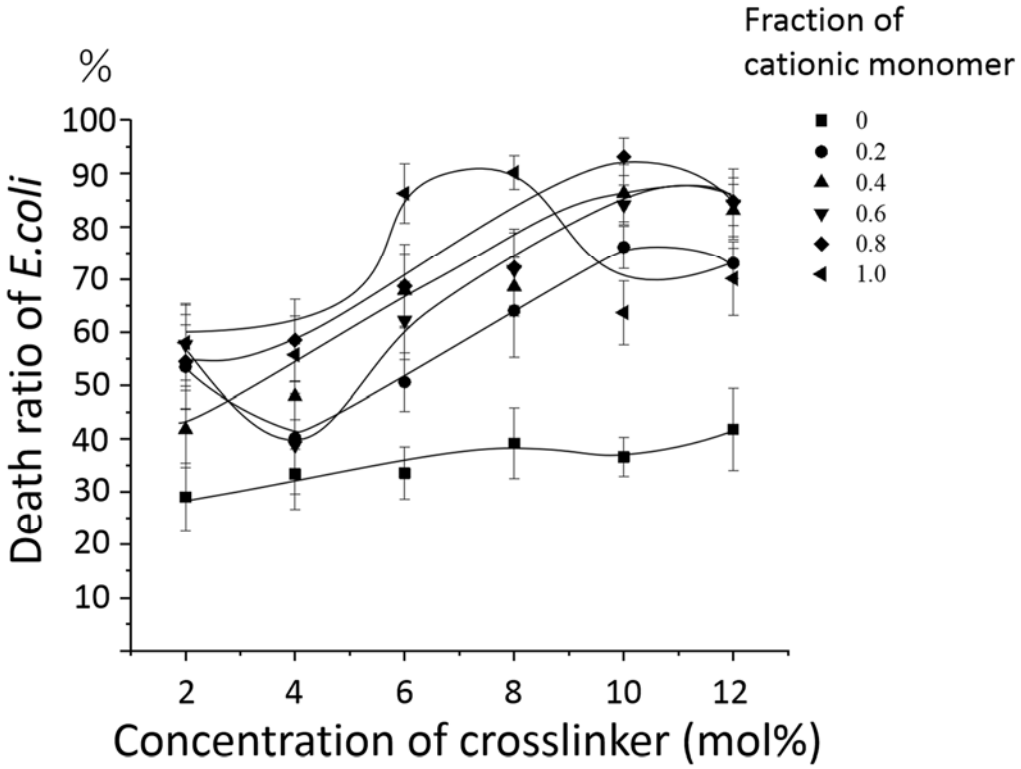

(Figure. 10) The death ratio of (a) *Escherichia coli* (*E. coli)* on copolymer hydrogels. Error bars indicate the standard deviation.

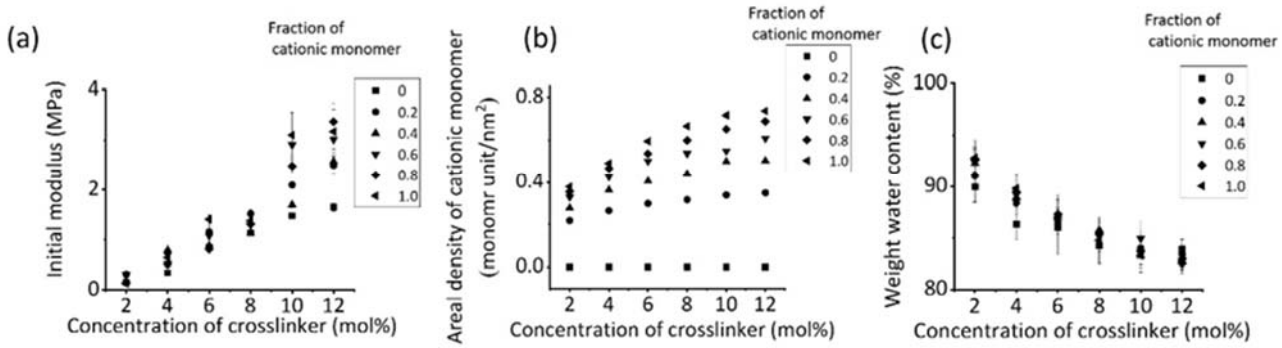

(Figure. 11) Correlation between cross-linker concentration, fraction of the cationic monomer, and physicochemical properties of copolymer hydrogels prepared from (3-acrylamidopropyl) trimethylammonium chloride (DMAPAA-Q) and N, N-dimethylacrylamide (DMAAm). (a) Initial elastic modulus of the hydrogels. (b) Areal density of the cationic monomer of the hydrogels. (c) Weight water content of the hydrogels.

5.3 Results and Discussion

The factors influencing the bactericidal effect of the cationic hydrogels were investigated by plotting the death ratio of *E. coli*. against the initial elastic modulus (Figure 12(a)), the water weight of the hydrogels (Figure 12(b)), and the areal density of the cationic monomers of the hydrogels (Figure 12(c)). The bacterial death ratio was not significantly correlated with the initial modulus and water content of the hydrogels; however, it was strongly correlated with the areal density of the cationic monomers, i.e., higher the areal density of the cationic monomers, stronger the bactericidal effect of the cationic hydrogels. Previous studies have suggested that hydrophilic cationic polymers share ionic interactions with plasma membrane molecules, and the incorporation of membrane molecules with the polymers disrupts the membrane assembly.[5,6] Indeed, studies on hydrogels and protein adsorption have reported that cationic hydrogels adsorb large amounts of anionic charged proteins. [7]

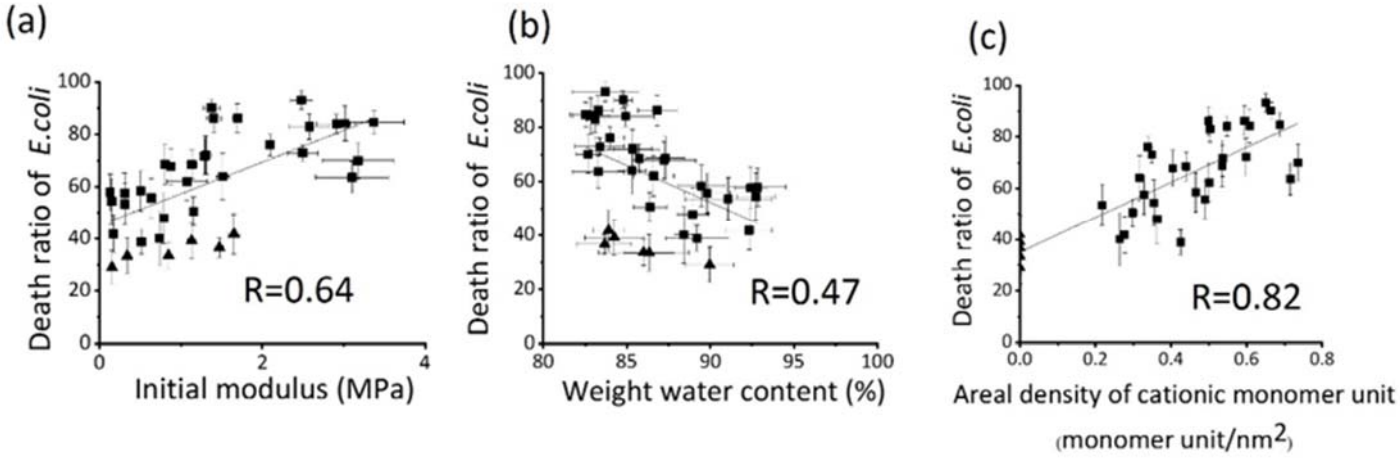

(Figure. 12) Death ratio of *Escherichia coli* (*E. coli)* on hydrogels as a function of the physicochemical properties of the hydrogel. (a) Initial modulus, (b) water weight of the hydrogels, (c) areal density of the cationic monomer of the hydrogels. Symbol ■ indicates hydrogels containing cationic polymers. Symbol ▲ indicates hydrogels containing only neutral polymers (zero fraction of the cationic monomer). R is the correlation coefficient.

5.4 References

(1) Hoshino, K.I.; Nakajima, T.; Matsuda, T.; Sakai T.; Gong, J.P. Network elasticity of a model hydrogel as a function of swelling ratio: from shrinking to extreme swelling states. *Soft Matter* **2018** *14*, 9693.

(2) Y. Hu; X. Zhao; J. J. Vlassak and Z. Suo Using indentation to characterize the poroelasticity of gels. Appl. Phys. Lett., 2010 96, 121904.

(3) C. T. McKee; J. A. Last; P. Russell and C. J. Murphy Indentation Versus Tensile Measurements of Young's Modulus for Soft Biological Tissues. Tissue Eng., Part B, 2011 17 (3), 155-164.

(4) D. C. Lin; D. I. Shreiber; E. K. Dimitriadis and F. Horkay Spherical Indentation of Soft Matter Beyond the Hertzian Regime: Numerical and Experimental Validation of Hyperelastic Models. Biomech. Model. Mechanobiol., 2009 8 (5), 345-358.

(5) Li, P.; Poon, Y.F.; Li, W.; Zhu, H.Y.; Yeap, S.H.; Cao, Y. Qi, X.; Zhou, C.; Lamrani, M.; Beuerman, R.W.; Kang, E.T.; Mu, Y.; Li, C.M.; Chang, M.W.; Jan Leong

S.S.; Chan-Park, M.B. A polycationic antimicrobial and biocompatible hydrogel with microbe membrane suctioning ability. *Nat. Mater.* **2011**, 10 (2), 149-156.

(6) Gabriel, G. J.; Som, A.; Madkour, A. E.; Eren, T. & Tew, G. N. Infectious disease: Connecting innate immunity to biocidal polymers. Mater. Sci. Eng. R 2007 57, 28–64.

(7) Guo H.; Uehara Y., Matsuda T.; Kiyama R.; Li L.; Ahmed J.; Katsuyama Y.; Nonoyama T.; Kurokawa T. Surface charge dominated protein absorption on hydrogels *Soft Matter* **2020**, 16, 1897

CHAPTER 6: Bactericidal effect of cationic polymers

6.1 Introduction

Previous experiments revealed that the bactericidal effect of cationic hydrogels is important to have cationic functional groups regardless of the monomer species.

In Chapter 6, we investigated whether PDMAPAA-Q has a bactericidal effect even in the uncrosslinked polymer state.

6.2 Material

6.2.1 Preparation of polymer

In this chapter, two types of polymers were used: PDMAPAA-Q as a cationic polymer and PDMAAm as a neutral polymer. Each monomer solution was prepared with a monomer concentration of 2 M and an initiator concentration of 0.1 mol% and subjected to UV polymerization in an argon atmosphere for 8 hours. The polymer solution was dialyzed with stirring in pure water for 5 days using a semipermeable membrane to remove unpolymerized monomers. They then used a vacuum oven to remove the moisture from the polymer solution and pulverized it into a polymer powder for use in the experiment.

6.2.2 Preparation of bacterial strain

In this experiment, *E. coli* was used as the species. The bacterial suspension was prepared by 2.4 methods.

6.3 Method

6.3.1 Antibacterial test

In this chapter, after sterilization testing, E. coli was stained with a fluorescent dye and mortality of E. coli was measured using a fluorospectro-photometer. First, the polymer powder was added in physiological saline at concentrations of 1 M, 0.75 M, 0.5 M, and 0.25 M, and sterilized in an autoclave. Thereafter, the prepared fungal solution was added to the polymer solution and left in an incubator (37 ° C) with stirring for 12 hours. Saline was then added to the solution to reduce the viscosity, and a fluorescent dye was added to stain E. coli. The death ratio of *E.coli* was calculated using a fluorospectro-photometer and a calibration curve.

6.3.2 Standard curve

After incubation of E. coli in LB liquid medium, the culture is divided into two parts. Both were washed with saline and one was sterilized with 70% ethanol. One bacterial fluid contains only live E. coli and the other bacterial fluid contains only dead E. coli. By mixing these two kinds of bacterial solutions, a bacterial solution containing 100%, 75%, 50%, 25% and 0% of dead E. coli was prepared and stained with a fluorescent dye. Fluorescence emission of the bacterial solution was measured by fluorospectro-photometer, and the areas of wavelength between 490 nm and 520 nm (Area (1)) and

600 nm and 630 nm (Area (2)) were calculated. Area (1) is the fluorescence emitted by live E. coli, and area (2) is the fluorescence emitted by dead E. coli. The standard curves were obtained by dividing the area of Area (1) by the area of Area (2). (Figure.13)

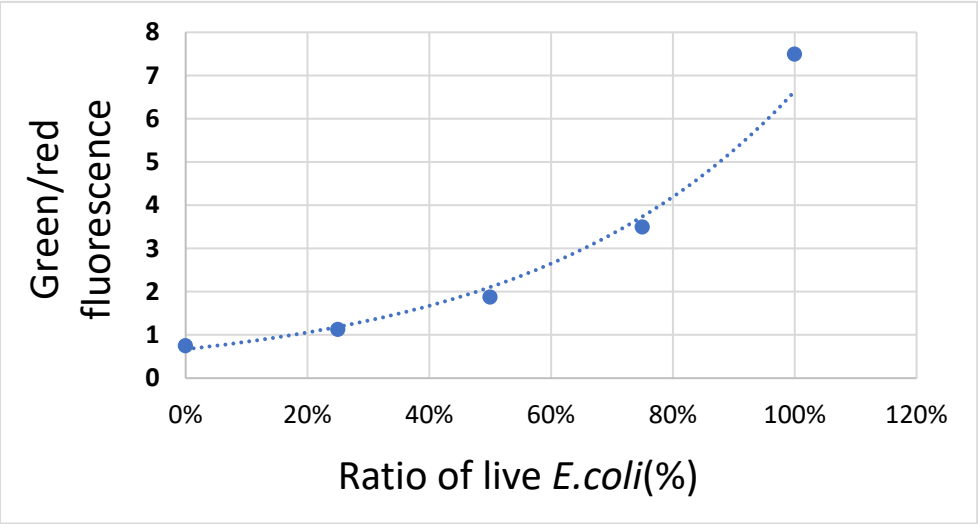

(Figure. 13) Standard curve of *E. coli*. The horizontal axis shows the percentage of viable *E.coli*. The vertical axis shows the value obtained by dividing Area (1) by Area (2).

6.4 Result and discussion

Most samples of cationic and neutral polymers showed less than 40% death ratio against *E.coli*. (Figure.14) Furthermore, the death ratio of *E. coli* in cationic polymers was compared with that of E. coli on cationic hydrogels. (Figure.15) The data of the cationic hydrogel used at this time were 1.0 samples of fraction of cationic monomer in Figure 11(b). As the result, it was clarified that the cationic polymer made from the same monomer species showed high bactericidal effect by crosslinking. The bactericidal mechanism of biguanide fungicides mentioned in the introduction is thought to be important to fix and inhibit cell membrane fluidity. It is considered that the cationic polymer can inhibit the flow of cell membrane more strongly than the polymer state by gelation with a crosslinking agent.

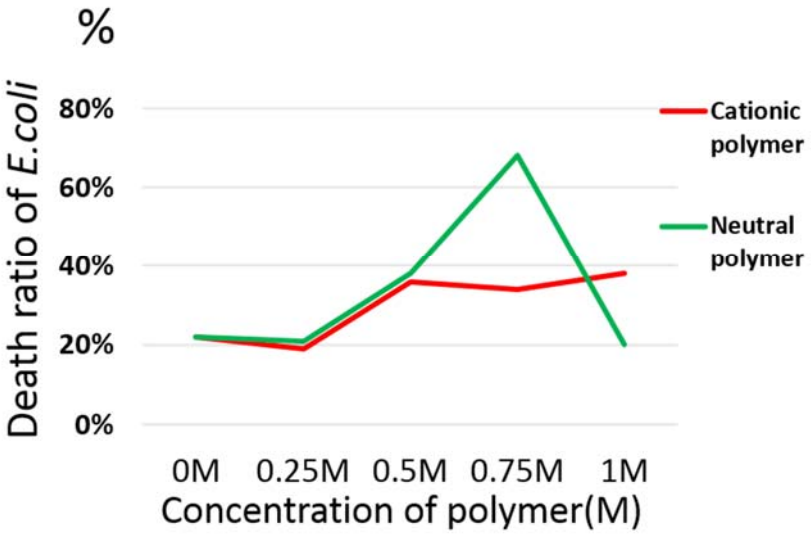

(Figure. 14) Death ratio of *E.coli* in cationic polymer solution (PDMAPAA-Q) and neutral polymer solution (PDMAAm)

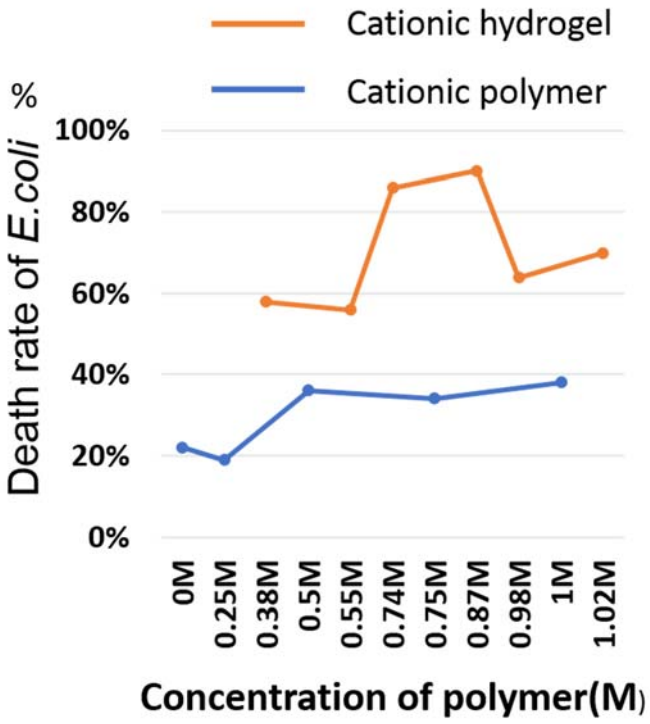

(Figure. 15) Death ratio of *E.coli* in cationic polymer solution and on cationic hydrogel.

CHAPTER 7: Disruption of bacterial cell membrane by cationic hydrogel

7.1 Introduction

From previous chapters, it has been suggested that contact between cationic hydrogels and bacterial cell membranes via ionic interactions is important for bactericidal effects.

In Chapter 5, the mechanism by which hydrogels are sterilized after contact with bacteria is discussed based on the physical properties of hydrogels. In this study, we focused on the elastic energy of the gel resulting from local deformation at ion-binding sites between the bacteria and hydrogels. The deformation of the hydrogel due to drying and the movement of the bacteria generate elastic energy at the ion-binding sites of the bacteria and the hydrogel. We considered that when elastic energy (W_{el}) exceeds the interfacial free energy (W_f) required to expose the hydrophobic ends of the lipid bilayer in solution, the lipid bilayer is considered to have been disrupted (Figure.16). In Chapter 5, it was discussed whether the theory of this sterilization mechanism was realistic by actually calculating elastic energy and comparing it with the interfacial tension of cell membrane.

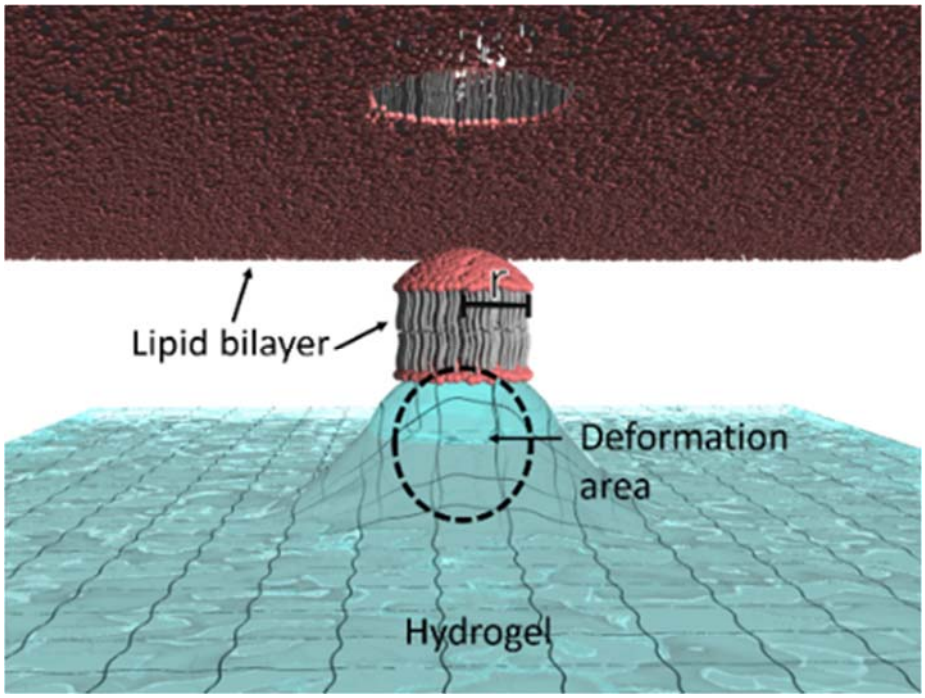

(Figure. 16) Schematic representation of the mechanism underlying the sterilization effect of the cationic hydrogels, involving the atrial elimination of lipid bilayers from the bacterial cell membranes.

7.2 Calculation of the elastic energy (W_{el}) of the gel

W_{el} (4) were estimated from the following equations. When calculating the local elastic energy, the deformation region of the hydrogel in which it occurs was assumed to be a sphere. The elastic energy is increased not only by the magnitude of the strain in the ion-binding region of the hydrogel and the bacterium but also by the expansion of the ion-binding region.

$$W_{el} = \frac{1}{2} E \varepsilon^2 * \frac{4}{3} \pi r^3 \quad ...(4)$$

Where, E, ε and r are the Young's modulus of the PDMAPAA-Q gel (monomer concentration, 2 M; cross-linker concentration, 6 mol%), the strain, and the radius of the contact area (m), respectively. Values of ε were set from 0.06 to 0.1.

7.3 Calculation of the interfacial free energy (W_f)

W_f (5) were estimated from the following equations.

$$W_f = 2(\gamma t 2\pi r) \quad ...(5)$$

Where, γ and t are the interfacial tensions of n-heptadecane ($53.2 N/m^2$) [1,2] and the length of the hydrophobic portion of a single phospholipid molecule that forms the bacterial lipid bilayer(2.13nm), respectively. The interfacial energy (W_f) determined herein was doubled because two hydrophobic regions (r) were formed upon detachment of the cell membrane. The W_f calculated by this equation was the value required to

remove the entire lipid bilayer structure where the cell and hydrogel are bound to ionic interactions from the cell membrane. The reason why the whole bilayer structure was chosen as the target for the destruction of the plasma membrane was that it requires less energy to pull out the entire bilayer structure than to pull out only mono layer of the lipid bilayers.

7.4 Result and discussion

A graph of r on the horizontal axis and W on the vertical axis was plotted on the basis of equations (4) and (5) (Figure.17). The graph shows that W_{el} exceeds W_f when r increases and exceeds a certain value. With an increase in ε, W_{el} exceeds W_f in a smaller adsorption area. In other words, the membrane can be disrupted with an adsorption radius of several tens of nanometers. These findings indicate that cationic hydrogels strongly bind to bacteria through their cationic charges, and the contact area between the bacteria and the hydrogel was gradually increased. This ion-binding region was considered to have been eliminated from the bacterial cell membrane owing to certain factors.

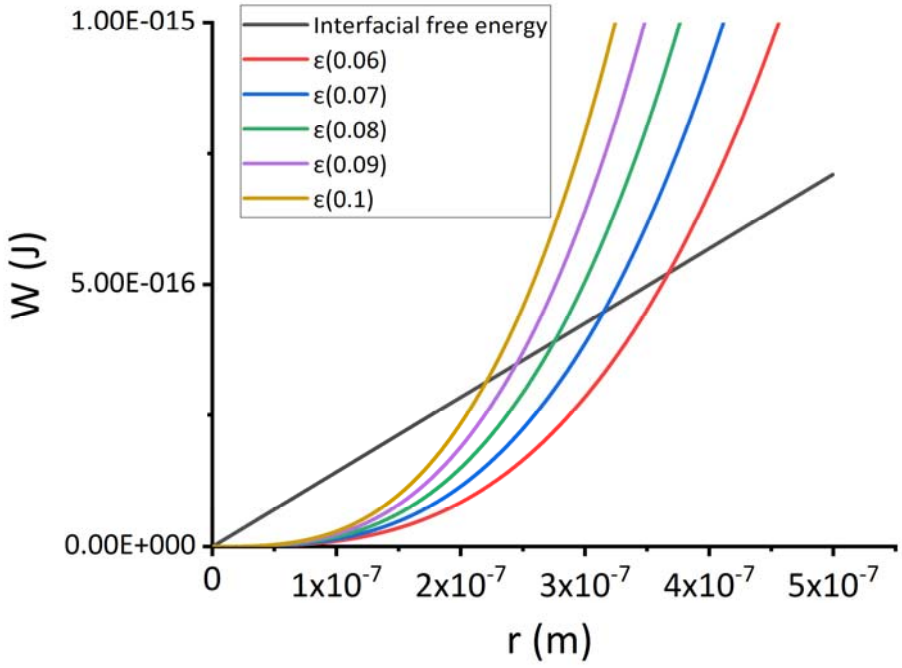

(Figure. 17) Dependence of cell membrane interfacial energy and hydrogel elastic energy [W (J)] on adsorption radius between the bacteria and the hydrogel [r (m)].

7.5 Ion binding energy in the contact area

It was clarified that the elastic energy (W_{el}) exceeded The interfacial energy (W_f) in the realistic value in chapter 7.4. Next, we examined whether the energy of the ionic bond of the contact region between the cell membrane and cationic hydrogel exceeded W_{el} when the cell membrane was pulled out by cationic hydrogel. The value of the energy of the ionic bond in physiological saline solution (E_a=1.7E-20(J)) was cited from the reference[3].

From figure 17, when the strains were 0.06 and 0.1, the contact area was calculated using the adsorption radius (r) at which W_{el} exceeded W_f. The values of areal density of the cationic monomer unit from Figure 10 (b) were used. From r and the values of areal density of the cationic monomer unit, the number of cationic monomer unit in the contact area was calculated. Then, the energy of the ionic bond in the contact area was calculated from the value of the energy of the ionic bond in the physiological saline and the number of cationic monomer unit.

As a result, when the strain was 0.06, the ion binding energy in the contact area when W_{el} exceeded W_f was 4.3 E -15 (J). This value was found to be stronger than W_{el} (5.2E-16 J) in this condition. when the strain was 0.1, the ion binding energy in the contact area when W_{el} exceeded W_f was 1.5 E -15 (J). This value was also stronger than W_{el}

(5.2E-16 J). This suggests that the ionic bond does not break before the hydrogel abstracts the cell membrane.

7.6 References

(1) Rehfeld, S.J. Adsorption of sodium dodecyl sulfate at various hydrocarbon-water interfaces *J. Phys. Chem.* 1967 *71*, 738-745.

(2) Tuan, V.; Vu, D. Synergistic effects of surfactants and heterogeneous nanoparticles at oil-water interface: Insights from computations. Journal of Colloid and Interface Science. 2019 *553* (1), 50-58.

(3) Evan, S.; Sebastiaan, A. Direct Measurement of the Strength of Single Ionic Bonds between Hydrated Charges. ACS. NANO, 2012,6, (6), 5297-5303.

CHAPTER 8: Summary of the dissertation

In this paper, to investigate the bactericidal activity of cationic hydrogel, bacteria were seeded on the cationic hydrogel, and their life and death were observed by time lapse. When the characteristic sterilization time of the cationic hydrogel was calculated by making the survival curve of the bacterium, the bactericidal time was about 6 hours for the gram-negative bacterium and about 7 hours for the gram-positive bacterium. It was clarified from this result that the sterilization effect was shown by the contact with bacteria for a long time in the cationic hydrogel.

In chapter 4, we evaluated the bactericidal effects of cationic hydrogels. Cationic hydrogel, neutral hydrogel, and agar which was negative control were prepared, on which bacteria were seeded and allowed to stand for a fixed time. When the survival ratio of the bacteria was compared afterwards, the cationic hydrogel showed high bactericidal effect.

In chapter 5, we examined the relationship between the physical properties of hydrogels and their bactericidal effects. A plurality of composite hydrogels prepared from cationic monomers and neutral monomers having different physical properties were prepared, and their sterilization effects were evaluated. The areal density of the cationic monomers showed a high correlation with the Death ratio of bacteria. We considered that ionic bonding by cationic charge of hydrogel and anionic charge of cell membrane plays an important role in bactericidal effect.

Furthermore, in Chapter 6, the bactericidal effect of cationic polymers was measured and compared with that of cationic hydrogels, suggesting that gelation with a crosslinking agent enhances the bactericidal effect.

Next, the mechanism of sterilization after ion binding was discussed from the viewpoint of elastic energy generated in the binding region and interfacial tension of the cell membrane. As a result, it was clarified that the the elastic energy (W_{el}) increased as the binding region between the cell membrane and hydrogel increased or the strain increased and exceeded the interfacial energy (W_f) of the cell membrane at a realistic value. When the W_{el} exceeds the W_f, the ion binding region is pulled out from the cell membrane, and the cell membrane is destroyed.

In this paper, it was shown that the sterilization effect could be easily given to the hydrogel by using the cationic monomer. And, it is considered that a large contribution can be made to future research on sterilization by examining the sterilization mechanism from the viewpoint of the elastic energy which is not conventional.

List of Publications

Original papers related to doctoral dissertation

(1) Yuki Shibata, Takayuki Kurokawa, Tomoyasu Aizawa, Jian Ping Gong:

"Bactericidal effect of cationic hydrogels prepared from hydrophilic polymers"

Journal applied polymer sci 誌、Accepted

Presentation in conferences related to doctoral dissertation

(1) Yuki Shibata, Takayuki Kurokawa, Tomoyasu Aizawa, Jian Ping Gong : "Antibacterial property of cationic hydrogel" Gelsympo 2018, 4dMS (日本)

Acknowledgement

This research on this dissertation has been carried out in the Laboratory of Soft and Wet Matter (LSW), Graduate School of Life Science, Hokkaido University, Japan, supervised by Professor Takayuki Kurokawa. Associate examiners are Professor Jian Ping Gong, Professor Tomoyasu Aizawa.

Firstly, I greatly appreciate all the support and encouragement of my respected supervisor, Professor Takayuki Kurokawa during master's and doctoral study in LSW. He gave me not only tremendous academic support to be an outstanding researcher but also so many wonderful opportunities. I really appreciate that he evaluated my doctoral research, and through a lot of discussions with him, I could acquire a deep understanding of polymer materials and an ability to perform research. I really respect his positive attitude, research understanding and considering.

I would like to many thanks also to Professor Jian Ping Gong, Professor Tomoyasu Aizawa, Associate Professor Tasuku Nakajima, Assistant Professor Takayuki Nonoyama for their helpful scientific comments, discussions and suggestions regarding my research. I am also very grateful to post-doctoral fellows, guest researcher and

research assistants in “LSW”. I also would like to thank the staffs in LSW; Ms. Eiko Hasegawa, Ms. Yuki Okubo, Ms. Kato and Ms. Iseya for helping me in financial works and lab life of Hokkaido University.

Finally, special thanks to my family for all the support and encouragement during the life in Hokkaido University. I dedicate this dissertation to them.

Yuki Shibata

Laboratory of Soft & Wet Matter

Graduate School of Life Science

Hokkaido University

Sapporo Japan

September 2020